its function by affecting ATP binding (*11*). Thus, the F548L polymorphism is expected to reduce the ability of $Pmr1^{BY}$ to transport manganese into the Golgi, relative to $Pmr1^{RM}$, consistent with BY's manganese sensitivity.

Pmr1 leucine-548 is conserved across fungi, with some species having an isoleucine or valine at the homologous position and none with phenylalanine (fig. S5). In the *S. cerevisiae* population, almost all sequenced *PMR1* alleles have leucine-548, with phenylalanine-548 found only in BY and other laboratory strains (*12*, *13*) whose PMR1 alleles are likely directly related to BY (*14*). BY is derived from EM93, a diploid strain isolated from a fig (*15*). Sequencing of *PMR1* in EM93 revealed that EM93 is heterozygous for Pmr1-F548L (fig. S6), suggesting that either the mutation is not laboratory-derived or that it occurred between EM93's isolation and its entry into a stock collection.

Decades of mapping studies have uncovered loci for myriad traits, but identification of the underlying genes and variants has lagged. Our CRISPR-assisted mapping approach promises to close this gap. In contrast to previous strategies, our method generates a higher density of recombination events, is easily targetable to any region of the genome, and does not require time-consuming extra generations of crossing to increase recombination frequency. Conversely, the strength of a traditional meiotic mapping panel is the ability to scan the entire genome. Complex traits, with multiple small-effect QTLs, pose a greater challenge for any mapping method. Importantly, in LOH mapping the rest of the genome outside the region targeted for LOH is held constant when a given QTL is being queried, thus effectively reducing the complexity of a trait by eliminating variance due to other segregating QTLs.

We anticipate that trait mapping with targeted LOH panels will aid efforts to understand the genetic basis of trait variation. In addition to applications in single-celled organisms, LOH panels could be generated from cultured cells, enabling in vitro genetic dissection of human traits with cellular phenotypes. In multicellular organisms, mapping resolution could be enhanced with CRISPR-directed meiotic recombination events. Indeed, the mutagenic chain reaction system developed in vivo in fruit flies (*16*) and mosquitos (*17*, *18*) uses CRISPR to generate gene conversion events in meiosis with high efficiency. Additionally, LOH in early development could generate chimeric individuals. The targeted LOH method also has the potential to be applied to viable interspecies hybrids that cannot produce offspring, allowing trait variation between species to be studied genetically beyond the few systems where it is currently possible (*19*, *20*).

In addition to their research applications, targetable endonucleases hold promise for gene therapy (*21*, *22*). Certain disease alleles may be difficult to directly target by CRISPR because of their sequence complexity, such as the expanded trinucleotide repeats that underlie Huntington's disease. In these cases, directing a DSB to occur in the vicinity of a pathogenic allele so that it is replaced with its nonpathogenic counterpart by LOH may represent a more feasible alternative.

REFERENCES AND NOTES

1. Y. Yin, T. D. Petes, *PLOS Genet.* **9**, e1003894 (2013).
2. V. Henson, L. Palmer, S. Banks, J. H. Nadeau, G. A. Carlson, *Proc. Natl. Acad. Sci. U.S.A.* **88**, 6486–6490 (1991).
3. R. Laureau *et al.*, *PLOS Genet.* **12**, e1005781 (2016).
4. J. A. Doudna, E. Charpentier, *Science* **346**, 1258096 (2014).
5. Materials and methods are available as supplementary materials on *Science* Online.
6. J. St. Charles, T. D. Petes, *PLOS Genet.* **9**, e1003434 (2013).
7. J. S. Bloom, I. M. Ehrenreich, W. T. Loo, T.-L. V. Lite, L. Kruglyak, *Nature* **494**, 234–237 (2013).
8. V. C. Culotta, M. Yang, M. D. Hall, *Eukaryot. Cell* **4**, 1159–1165 (2005).
9. M. Hilge *et al.*, *Nat. Struct. Biol.* **10**, 468–474 (2003).
10. C. Toyoshima, T. Mizutani, *Nature* **430**, 529–535 (2004).
11. J. D. Clausen, D. B. McIntosh, B. Vilsen, D. G. Woolley, J. P. Andersen, *J. Biol. Chem.* **278**, 20245–20258 (2003).
12. G. Liti *et al.*, *Nature* **458**, 337–341 (2009).
13. G. Song *et al.*, *PLOS ONE* **10**, e0120671 (2015).
14. J. Schacherer, J. A. Shapiro, D. M. Ruderfer, L. Kruglyak, *Nature* **458**, 342–345 (2009).
15. R. K. Mortimer, J. R. Johnston, *Genetics* **113**, 35–43 (1986).
16. V. M. Gantz, E. Bier, *Science* **348**, 442–444 (2015).
17. V. M. Gantz *et al.*, *Proc. Natl. Acad. Sci. U.S.A.* **112**, E6736–E6743 (2015).
18. A. Hammond *et al.*, *Nat. Biotechnol.* **34**, 78–83 (2016).
19. H. A. Orr, D. C. Presgraves, *BioEssays* **22**, 1085–1094 (2000).
20. G. C. Woodruff, O. Eke, S. E. Baird, M.-A. A. Félix, E. S. Haag, *Genetics* **186**, 997–1012 (2010).
21. P. Tebas *et al.*, *N. Engl. J. Med.* **370**, 901–910 (2014).
22. P. D. Hsu, E. S. Lander, F. Zhang, *Cell* **157**, 1262–1278 (2014).

ACKNOWLEDGMENTS

We thank Kruglyak laboratory members for helpful discussion, S. Clarke for strain BY4742, G. Church for plasmids, and S. Kosuri for his flow cytometer. Funding was provided by the Howard Hughes Medical Institute and NIH grants R01 GM102308 (L.K.) and F32 GM116318 (M.J.S). Sequencing data was deposited at the Sequence Read Archive under accession no. SRP072527, and other data and code was deposited at https://github.com/joshsbloom/crispr_loh.

SUPPLEMENTARY MATERIALS

www.sciencemag.org/content/352/6289/1113/suppl/DC1
Materials and Methods
Figs. S1 to S7
Tables S1 and S2
References (*23*–*36*)

19 February 2016; accepted 25 April 2016
Published online 5 May 2016
10.1126/science.aaf5124

MUCOSAL IMMUNOLOGY

Gene-microbiota interactions contribute to the pathogenesis of inflammatory bowel disease

Hiutung Chu,[1]* Arya Khosravi,[1] Indah P. Kusumawardhani,[1] Alice H. K. Kwon,[1] Anilton C. Vasconcelos,[2] Larissa D. Cunha,[3] Anne E. Mayer,[4] Yue Shen,[1] Wei-Li Wu,[1] Amal Kambal,[4] Stephan R. Targan,[5] Ramnik J. Xavier,[6] Peter B. Ernst,[2] Douglas R. Green,[3] Dermot P. B. McGovern,[5] Herbert W. Virgin,[4] Sarkis K. Mazmanian[1]*

Inflammatory bowel disease (IBD) is associated with risk variants in the human genome and dysbiosis of the gut microbiome, though unifying principles for these findings remain largely undescribed. The human commensal *Bacteroides fragilis* delivers immunomodulatory molecules to immune cells via secretion of outer membrane vesicles (OMVs). We reveal that OMVs require IBD-associated genes, *ATG16L1* and *NOD2*, to activate a noncanonical autophagy pathway during protection from colitis. ATG16L1-deficient dendritic cells do not induce regulatory T cells (T_{regs}) to suppress mucosal inflammation. Immune cells from human subjects with a major risk variant in *ATG16L1* are defective in T_{reg} responses to OMVs. We propose that polymorphisms in susceptibility genes promote disease through defects in "sensing" protective signals from the microbiome, defining a potentially critical gene-environment etiology for IBD.

Intestinal microbiota modulate development and function of the immune system and play a critical role in inflammatory bowel disease (IBD), a family of idiopathic intestinal disorders including Crohn's disease (CD) and ulcerative colitis (UC) (*1*–*6*). Concordance rates of 40 to 50% between monozygotic twins implicate gene-environment interactions in the pathogenesis of CD (*7*–*10*), albeit in ways that are poorly understood. Advances in DNA-sequencing technologies have empowered unprecedented insights into the human genome and the gut microbiome in IBD, enabling detailed genomic characterization of patients (*11*) and chronicling alterations in the composition and gene content of the gut microbiome (dysbiosis) (*12*).

[1]Division of Biology and Biological Engineering, California Institute of Technology, Pasadena, CA 91125, USA. [2]Center for Veterinary Sciences and Comparative Medicine, University of California, San Diego, San Diego, CA 92093, USA. [3]Department of Immunology, St. Jude Children's Research Hospital, Memphis, TN 38105, USA. [4]Department of Pathology and Immunology, Washington University School of Medicine, St. Louis, MO 63110, USA. [5]F. Widjaja Foundation Inflammatory Bowel and Immunobiology Research Institute, Cedars-Sinai Medical Center, Los Angeles, CA 90048, USA. [6]Gastrointestinal Unit and Center for the Study of Inflammatory Bowel Disease, Massachusetts General Hospital and Harvard Medical School, Boston, MA 02114, USA.
***Corresponding author. Email: hiuchu@caltech.edu (H.C.); sarkis@caltech.edu (S.K.M.)**

Close to 200 risk loci have been proposed for CD, with several susceptibility genes linked to the regulation of autophagy (e.g., autophagy-related 16–like 1, *ATG16L1*) (*13*–*15*) or to microbial sensors that activate autophagy [e.g., nucleotide-binding oligomerization domain–containing protein 2 (*NOD2*)] (*16*–*18*). Although previous studies have shown that disruption of ATG16L1 and NOD2 affects CD susceptibility through defects in microbial clearance (*19*–*23*), recent reports reveal that immune cells impaired in autophagy are hyperinflammatory (*24*–*29*). This suggests that deficiencies in ATG16L1 or NOD2 may contribute to CD risk through impaired anti-inflammatory responses, a hypothesis not mutually exclusive with microbial clearance functions.

The microbiome of CD patients is altered, with emerging evidence for cause-and-effect relationships to disease. Among other recent examples of host-microbe interactions (*3*, *5*, *6*), the human commensal *Bacteroides fragilis* has evolved beneficial immunomodulatory properties. During colonization of mice, *B. fragilis* capsular polysaccharide A (PSA) is packaged in outer membrane vesicles (OMVs) and delivered to intestinal dendritic cells (DCs) to induce interleukin-10 (IL-10) production from $CD4^+Foxp3^+$ regulatory T cells (T_{regs}), which protects from experimental colitis (*30*–*32*). To explore gene-environment interactions during host-microbiota symbiosis, we tested if genetic pathways linked to CD are involved in the immune response to *B. fragilis* OMVs.

Bone marrow–derived DCs (BMDCs) differentiated from wild-type (WT) and ATG16L1-deficient (*Atg16l1*$^{f/f1}$ *Cd11c-Cre*; *Atg16l1*$^{\Delta Cd11c}$) mice were pulsed with OMVs harvested from wild-type *B. fragilis* (WT-OMV), or an isogenic mutant lacking PSA (ΔPSA-OMV), and cocultured with $CD4^+$ T cells. As previously reported (*33*), WT-OMVs, but not vehicle or ΔPSA-OMVs, promote IL-10 production (Fig. 1, A to C, and fig. S1). Conversely, ATG16L1-deficient DCs do not support IL-10 production in response to WT-OMVs (Fig. 1, A to C). We observe similar results using *Atg16l1*$^{f/f1}$ *LysM-Cre* mice (fig. S3). Purified PSA does not require ATG16L1 for its activity (Fig. 1, A and C, and fig. S2). Next, we tested functional outcomes using in vitro T cell suppression assays. T_{regs} isolated from cocultures with *Atg16l1*$^{\Delta Cd11c}$ BMDCs treated with *B. fragilis* OMVs exhibit impaired suppressive activity (Fig. 1D and fig. S2A). Neither WT-OMVs nor pure PSA have any effect on IL-10 production among $CD4^+Foxp3^-$ type 1 regulatory T cells (fig. S4). ATG16L1, ATG5, and ATG7 are components of the autophagy elongation complex; BMDCs deleted in these genes likewise do not induce IL-10 production from T_{regs} (fig. S5). Further, recent reports reveal a role for autophagy components in T_{reg} homeostasis (*34*, *35*). Our findings indicate that ATG16L1-deficient DCs fail to respond to *B. fragilis* OMVs, demonstrating that autophagy components in DCs are required for commensal-driven T_{reg} induction and function.

ATG16L1, ATG5, and ATG7 participate in both canonical and noncanonical autophagy pathways (*36*). Interestingly, the classical autophagy-specific genes *Ulk1*, *Fip200*, or *Atg14* are not required for $CD4^+Foxp3^+IL\text{-}10^+$ T_{reg} induction upon WT-OMV treatment (fig. S6). We hypothesized that OMVs use the noncanonical autophagy pathway, LC3-associated phagocytosis (LAP), which is specifically activated by microbial ligands delivered as particles rather than as soluble molecules. LAP

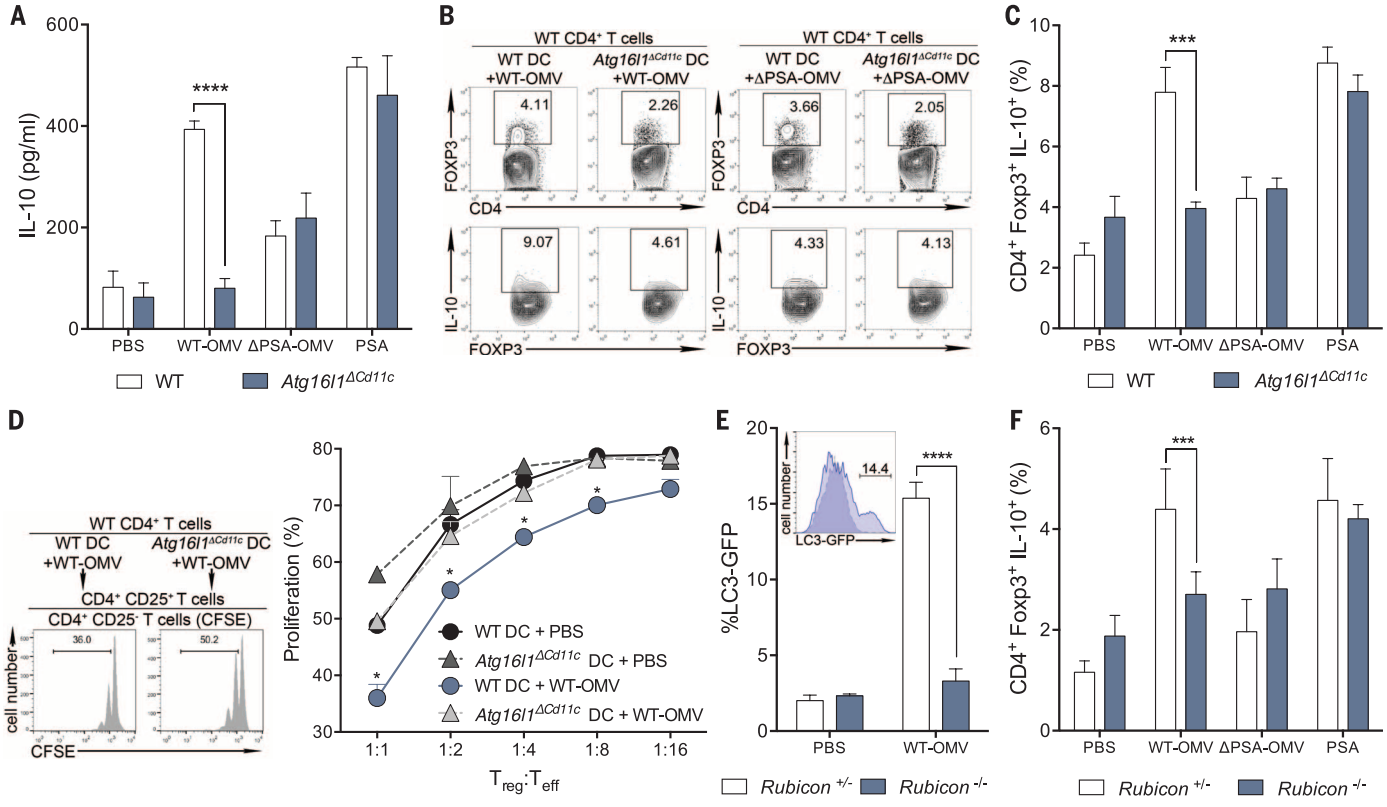

Fig. 1. ATG16L1 signals via a noncanonical autophagy pathway during OMV-mediated T_{reg} induction. (**A**) Enzyme-linked immunosorbent assay for IL-10 production during DC–T cell cocultures with WT or *Atg16l1*$^{\Delta Cd11c}$ BMDCs treated with phosphate-buffered saline (PBS), *B. fragilis* WT-OMV, ΔPSA-OMV, or purified PSA. (**B** and **C**) Representative flow cytometry plots (B) and frequency (C) of $CD4^+Foxp3^+IL\text{-}10^+$ T_{regs} from DC–T cell cocultures with WT or *Atg16l1*$^{\Delta Cd11c}$ DCs treated with PBS, *B. fragilis* WT-OMV, ΔPSA-OMV, or purified PSA. (**D**) T cell suppression assay analyzing in vitro–generated T_{regs} from WT or *Atg16l1*$^{\Delta Cd11c}$ DCs treated with WT-OMVs. (**E**) Quantification of LC3-GFP accumulation by *B. fragilis* WT-OMV treatment of *Rubicon*$^{+/-}$ or *Rubicon*$^{-/-}$ DCs. Representative flow cytometry histogram plot (inset). PBS, gray; WT-OMV, blue. (**F**) Frequency of $CD4^+Foxp3^+IL\text{-}10^+$ T_{regs} from *Rubicon*$^{+/-}$ or *Rubicon*$^{-/-}$ DC–T cell cocultures treated with PBS, *B. fragilis* WT-OMV, ΔPSA-OMV, or purified PSA. Error bars represent SEM. *$P < 0.05$, ***$P < 0.001$, ****$P < 0.0001$. Two-way analysis of variance (ANOVA), followed by Tukey's post-hoc analysis. Data are representative of at least two independent experiments.

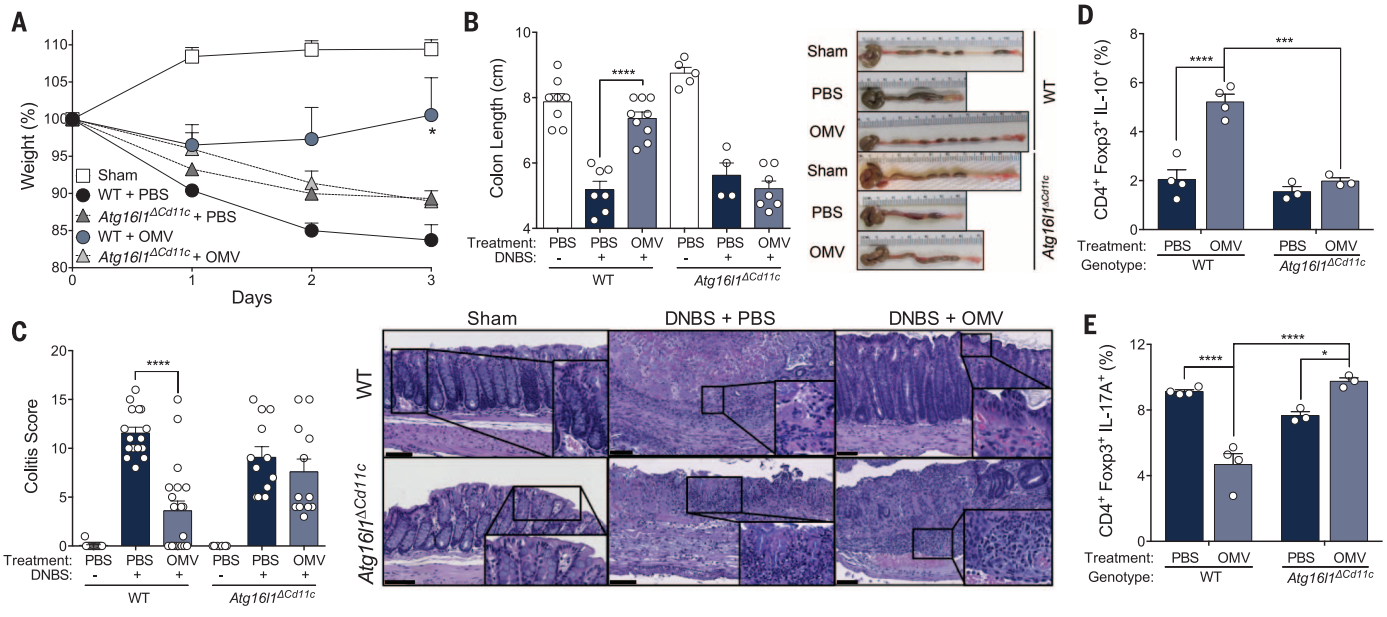

Fig. 2. *B. fragilis* OMVs require ATG16L1 in CD11c$^+$ DCs for protection from colitis. (**A** and **B**) Weight loss (A), colon length, and gross pathology (B) of WT and *Atg16l1*$^{\Delta Cd11c}$ mice orally treated with PBS or *B. fragilis* WT-OMV during DNBS colitis. Sham groups were treated with ethanol. (**C**) Colitis scores by a blinded pathologist using a standard scoring system, and representative hematoxylin and eosin (H&E) images. Scale bar, 100 μm. (**D** and **E**) MLN lymphocytes isolated post-DNBS analyzed for IL-10 (D) and IL-17A (E) production among CD4$^+$Foxp3$^+$ T_{regs}, as assessed by flow cytometry. Error bars represent SEM. *P < 0.05, ***P < 0.001, ****P < 0.0001. Two-way ANOVA, followed by Tukey's post-hoc analysis. Data are representative of at least three independent experiments, with three to nine mice per group.

activation requires RUBICON, which represses canonical autophagy (*36*). *Rubicon*$^{+/-}$ but not *Rubicon*$^{-/-}$ BMDCs display increased accumulation of lipidated, membrane-bound LC3-GFP (green fluorescent protein) (LC3-II) upon *B. fragilis* WT-OMV treatment (Fig. 1E). As expected, neither ΔPSA-OMVs nor purified PSA are able to activate LAP (fig. S7). Moreover, treatment of *Rubicon*$^{-/-}$ DCs fails to induce T_{reg} responses (Fig. 1F). As RUBICON is upstream of ATG16L1 signaling, OMVs preferentially use the noncanonical autophagy pathway LAP to mediate tolerogenic responses to *B. fragilis*. Further, these data suggest a reconsideration of previous literature assigning the role of ATG16L1 in IBD to defects exclusively in autophagy.

As a CD-risk gene, we investigated the in vivo requirement for ATG16L1 in CD11c$^+$ DCs during OMV-mediated protection from experimental colitis. Indeed, WT mice treated by oral gavage with WT-OMVs are protected from 2,4-dinitrobenzenesulfonic acid (DNBS) colitis (*33*), whereas *Atg16l1*$^{\Delta Cd11c}$ mice exhibit acute weight loss and increased mortality similar to that of untreated mice (Fig. 2A and fig. S8A). WT, but not *Atg16l1*$^{\Delta Cd11c}$, mice orally administered OMVs are protected from shortening of the colon, a hallmark of colitis models (Fig. 2B), with colitis scoring and cytokine profiles verifying protection from disease (Fig. 2C and fig. S8B). Prevention of colitis is not due to an overall defect in T_{reg} development in *Atg16l1*$^{\Delta Cd11c}$ mice (fig. S9). Further, although proportions of CD4$^+$Foxp3$^+$ cells are comparable in all groups of mice during colitis (fig. S10), *Atg16l1*$^{\Delta Cd11c}$ mice produce significantly less IL-10 from gut Foxp3$^+$ T_{regs} compared to WT mice after WT-OMV treatment (Fig. 2D and fig. S8C). Thus, WT-OMVs require ATG16L1 within DCs to induce IL-10 expression from Foxp3$^+$ T_{regs} and to suppress intestinal inflammation in a colitis model.

In addition to impaired IL-10 production in response to OMV treatment, *Atg16l1*$^{\Delta Cd11c}$ mice display an increase in IL-17A expression (Fig. 2E), but not IFN-γ (fig. S11), among mucosal CD4$^+$Foxp3$^+$ T cells during colitis. Further, in vitro cocultures of OMV-pulsed *Atg16l1*$^{\Delta Cd11c}$ BMDCs result in impaired IL-10 expression among T_{regs} (Fig. 1C) and increased IL-17A production in CD4$^+$Foxp3$^+$ T cells (fig. S12). Interestingly, whereas OMVs from other enteric bacteria each elicited a unique ATG16L1-dependent immune profile, only *B. fragilis* OMVs exclusively induce an anti-inflammatory response (fig. S13). Together, these data suggest that ATG16L1 deficiency in DCs alters the quality of the T cell response to OMVs.

As DCs coordinate adaptive immunity, we sought to determine how *Atg16l1*$^{\Delta Cd11c}$ DCs are impaired in promoting tolerogenic responses. After OMV stimulation, we observe no differences by WT or *Atg16l1*$^{\Delta Cd11c}$ DCs in internalizing OMVs or in surface expression of major histocompatibility complex class II (MHC II), CD80, and CD86 (fig. S14) (*27*). However, stimulation with OMVs results in an increase transcription of multiple proinflammatory cytokines in *Atg16l1*$^{\Delta Cd11c}$ DCs compared to WT cells (fig. S15). These data are consistent with previous reports of a hyperinflammatory response in ATG16L1-deficient macrophages and DCs stimulated with other microbial ligands (*24*, *26*). Abrogation of T_{reg} responses by ATG16L1-deficient DCs is likely due to increased proinflammatory cytokine production, which may impair DC–T cell interactions. *Atg16l1*$^{\Delta Cd11c}$ mice do not display more severe colitis than WT mice in the absence of OMV treatment (Fig. 2), suggesting that lack of protection is not due to more fulminant inflammation, but rather to an inability to induce T_{regs} in mice deficient in ATG16L1 among CD11c$^+$ DCs.

NOD2 encodes an intracellular sensor of bacterial peptidoglycan, and polymorphisms in this gene contribute to the largest fraction of genetic risk for CD (*13*). NOD2 has been shown to physically recruit ATG16L1 (*20*, *21*), a process that is impaired in human cells homozygous for a *NOD2* frameshift mutation (*20*). Accordingly, *Nod2*$^{-/-}$ BMDCs pulsed with WT-OMVs are unable to support IL-10 production from Foxp3$^+$ T_{regs} during in vitro cocultures (Fig. 3, A and B), revealing a crucial role for NOD2 signaling in microbiome-mediated immune tolerance. This notion is supported by in vivo studies showing that *Nod2*$^{-/-}$ mice are not protected from colitis by WT-OMV treatment (Fig. 3, C and D). Similar to *Atg16l1*$^{\Delta Cd11c}$ animals, *Nod2*$^{-/-}$ mice produce significantly less IL-10 from Foxp3$^+$ T_{regs} of the mesenteric lymph node (MLN) after WT-OMV treatment (fig. S16A), and proportions of T_{regs} remain unchanged during DNBS colitis (fig. S16B). Previous studies have shown that Toll-like receptor 2 (TLR2) is required for the PSA response (*33*, *37*). Although the role of NOD2 in inducing LAP is currently unknown, signaling through TLR2 potently activates LAP (*36*, *38*). *B. fragilis* OMVs induce reactive oxygen species from WT DCs,

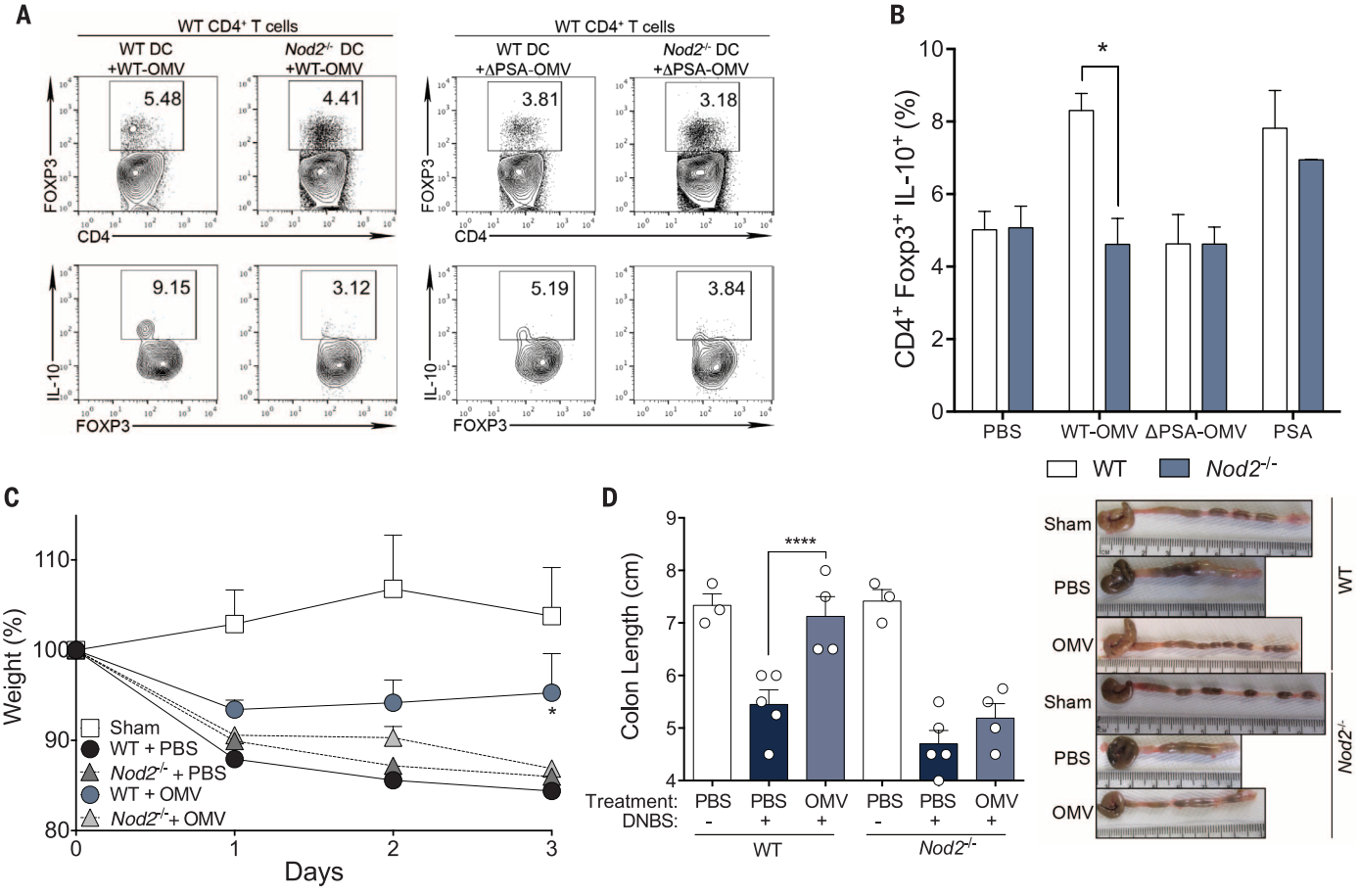

Fig. 3. NOD2 is required for OMV-mediated T_{regs} induction and protection from colitis. (**A** and **B**) Representative flow cytometry plots (A) from WT-OMV (left)– and ΔPSA-OMV (right)–treated BMDCs cocultured with $CD4^+$ T cells, and frequency (B) of $CD4^+Foxp3^+IL\text{-}10^+$ T_{regs} from DC–T cell cocultures. (**C** and **D**) Weight loss (C), colon length, and gross pathology (D) of WT or *Nod2*$^{-/-}$ mice treated with PBS or *B. fragilis* WT-OMV during DNBS colitis. Error bars represent SEM. *P < 0.05, ****P < 0.0001. Two-way ANOVA, followed by Tukey's post-hoc analysis. Data are representative of at least three independent experiments, with three to five mice per group.

a known product of LAP activation (*36*), but at significantly reduced levels in *Nod2*$^{-/-}$ or *Tlr2*$^{-/-}$ DCs (fig. S17). Though further studies are needed to define the mechanism of LAP activation by OMVs, these data reveal that *NOD2* and *ATG16L1* may cooperate as part of a common pathway to promote anti-inflammatory immune responses to the microbiome.

To extend and validate gene deletion approaches, we tested responses to OMVs by immune cells carrying the CD-associated variant of *ATG16L1* (*13*, *14*, *39*). The *ATG16L1* T300A variant leads to protein instability and altered cellular responses (*23*). BMDCs from transgenic mice expressing the T300A allele are also unable to promote IL-10 expression from $Foxp3^+$ T_{regs} in response to WT-OMVs (fig. S18A). Further, *ATG16L1* T300A transgenic mice are not protected from DNBS colitis and do not mount a potent T_{reg} response when administered WT-OMV compared to WT mice (fig. S18, B to G). These findings prompted us to investigate if human immune cells from CD patients with the *ATG16L1* T300A risk variant (table S1) are also defective in promoting $Foxp3^+$ T_{reg} development by *B. fragilis* OMVs. Monocyte-derived dendritic cells (MoDCs) from CD patients and healthy controls harboring either the protective allele (T300) or the risk allele (A300) were pulsed with OMVs or PSA and cocultured with syngeneic $CD4^+$ T cells. Consistent with our mouse data, human cells homozygous for the risk allele are unable to support induction of IL-10 from $Foxp3^+$ T_{regs} by WT-OMVs compared to MoDCs carrying the protective allele (Fig. 4). Notably, all samples tested display the predicted outcome based on genotype and not disease status. However, cells from most subjects, regardless of genotype, respond to purified PSA (Fig. 4). Collectively, we conclude that mouse and human DCs require functional ATG16L1 for induction of $CD4^+Foxp3^+IL\text{-}10^+$ T_{regs} in response to *B. fragilis* OMVs.

IBD affects more than 1.5 million people in the United States, with rates of diagnosis increasing and treatment options remaining limited (*40*, *41*). The etiology of IBD is complex and incompletely resolved (*1*). Here, we describe how interactions between genetic (*ATG16L1*/*NOD2*) and environmental (microbiome) factors cooperate to promote beneficial immune responses. *B. fragilis* OMVs use LAP, an ATG16L1-dependent cellular trafficking and signaling pathway, to induce mucosal tolerance. The hyperinflammatory responses that occur with mutations in *ATG16L1* likely alter antigen-processing pathways and impair signaling by DCs to T cells and may explain why CD-associated polymorphisms abrogate T_{reg} induction by OMVs. Collectively, discovery of genetic circuits co-opted by the microbiome to engender health provides unprecedented functional insights into gene-environment interactions relevant to the pathogenesis of IBD. We propose an additional role for genes previously implicated in killing bacteria—namely, mutations in genetic pathways linked to IBD result in an inability to sense and/or respond to beneficial microbes. This hypothesis may represent a new perspective for the etiology of microbiome-related diseases.

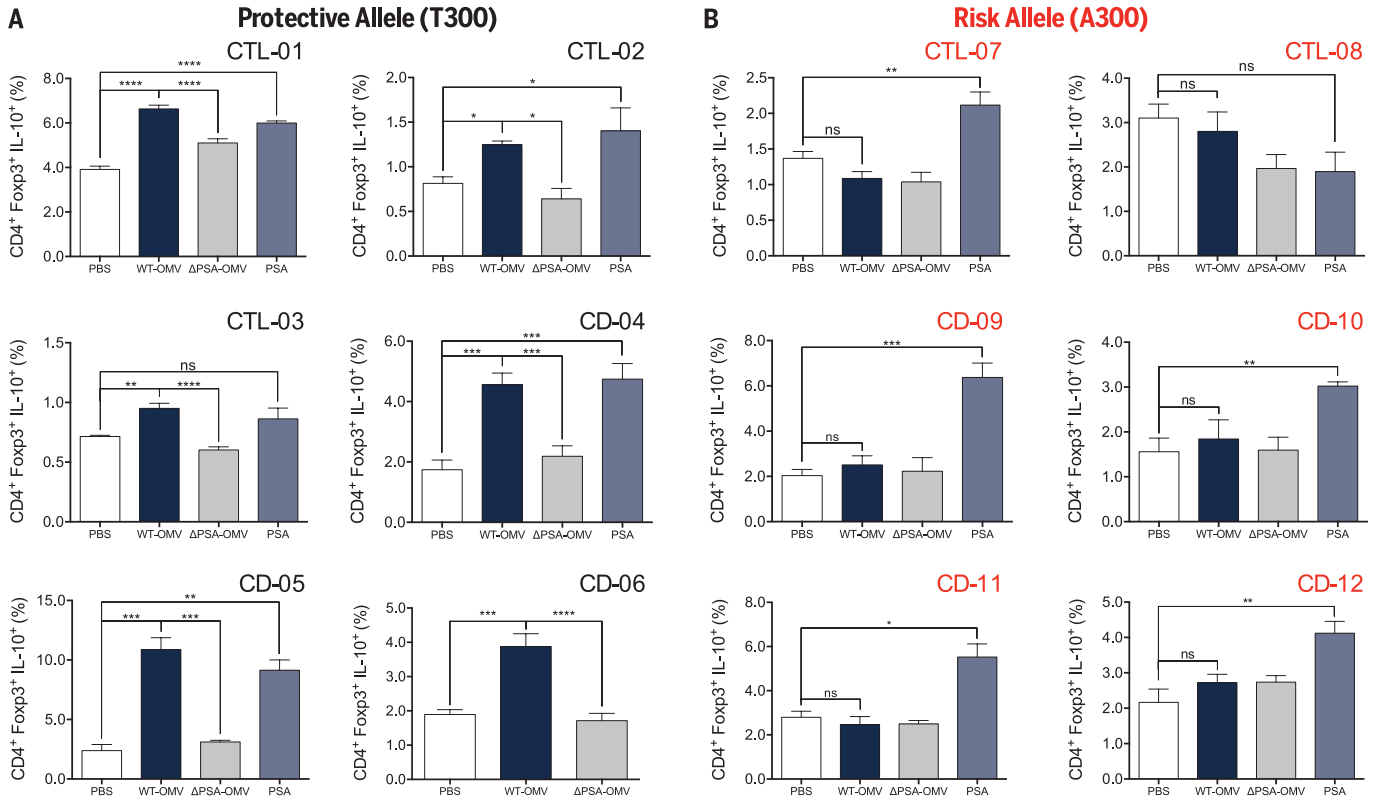

Fig. 4. The T300A risk variant of *ATG16L1* in human cells is unable to support OMV responses. (**A** and **B**) MoDCs with either the protective (A) or risk (B) allele were treated with PBS, *B. fragilis* WT-OMV, ΔPSA-OMV, or purified PSA; washed; and cocultured with syngeneic $CD4^+$ T cells. IL-10 expression was analyzed by flow cytometry among $CD4^+Foxp3^+$ T_{regs}. Human samples were processed and analyzed in a blinded fashion. CTL, control subjects; CD, Crohn's disease subjects. Error bars represent SEM. $^*P < 0.05$, $^{**}P < 0.01$, $^{***}P < 0.001$, $^{****}P < 0.0001$; ns, not significant. One-way ANOVA, followed by Tukey's post-hoc analysis.

REFERENCES AND NOTES

1. D. A. Peterson, D. N. Frank, N. R. Pace, J. I. Gordon, *Cell Host Microbe* **3**, 417–427 (2008).
2. D. A. Hill, D. Artis, *Annu. Rev. Immunol.* **28**, 623–667 (2010).
3. K. Honda, D. R. Littman, *Annu. Rev. Immunol.* **30**, 759–795 (2012).
4. E. M. Brown, M. Sadarangani, B. B. Finlay, *Nat. Immunol.* **14**, 660–667 (2013).
5. Y. Belkaid, T. W. Hand, *Cell* **157**, 121–141 (2014).
6. L. V. Hooper, D. R. Littman, A. J. Macpherson, *Science* **336**, 1268–1273 (2012).
7. S. R. Brant, *Inflamm. Bowel Dis.* **17**, 1–5 (2011).
8. M. Orholm *et al.*, *Scand. J. Gastroenterol.* **35**, 1075–1081 (2000).
9. J. Halfvarson, L. Bodin, C. Tysk, E. Lindberg, G. Järnerot, *Gastroenterology* **124**, 1767–1773 (2003).
10. C. Tysk, E. Lindberg, G. Järnerot, B. Flodérus-Myrhed, *Gut* **29**, 990–996 (1988).
11. L. Jostins *et al.*, *Nature* **491**, 119–124 (2012).
12. M. Wlodarska, A. D. Kostic, R. J. Xavier, *Cell Host Microbe* **17**, 577–591 (2015).
13. J. Hampe *et al.*, *Nat. Genet.* **39**, 207–211 (2007).
14. J. D. Rioux *et al.*, *Nat. Genet.* **39**, 596–604 (2007).
15. M. Parkes *et al.*, *Nat. Genet.* **39**, 830–832 (2007).
16. A. Gardet, R. J. Xavier, *Curr. Opin. Immunol.* **24**, 522–529 (2012).
17. J. P. Hugot *et al.*, *Nature* **411**, 599–603 (2001).
18. Y. Ogura *et al.*, *Nature* **411**, 603–606 (2001).
19. K. S. Kobayashi *et al.*, *Science* **307**, 731–734 (2005).
20. L. H. Travassos *et al.*, *Nat. Immunol.* **11**, 55–62 (2010).
21. R. Cooney *et al.*, *Nat. Med.* **16**, 90–97 (2010).
22. A. Murthy *et al.*, *Nature* **506**, 456–462 (2014).
23. K. G. Lassen *et al.*, *Proc. Natl. Acad. Sci. U.S.A.* **111**, 7741–7746 (2014).
24. T. Saitoh *et al.*, *Nature* **456**, 264–268 (2008).
25. K. Cadwell *et al.*, *Cell* **141**, 1135–1145 (2010).
26. V. M. Hubbard-Lucey *et al.*, *Immunity* **41**, 579–591 (2014).
27. S. Park *et al.*, *Cell Host Microbe* **19**, 91–101 (2016).
28. Q. Lu *et al.*, *Cell Host Microbe* **19**, 102–113 (2016).
29. J. M. Kimmey *et al.*, *Nature* **528**, 565–569 (2015).
30. S. K. Mazmanian, J. L. Round, D. L. Kasper, *Nature* **453**, 620–625 (2008).
31. J. L. Round, S. K. Mazmanian, *Proc. Natl. Acad. Sci. U.S.A.* **107**, 12204–12209 (2010).
32. S. E. Allan *et al.*, *Immunol. Rev.* **223**, 391–421 (2008).
33. Y. Shen *et al.*, *Cell Host Microbe* **12**, 509–520 (2012).
34. J. Wei *et al.*, *Nat. Immunol.* **17**, 277–285 (2016).
35. A. M. Kabat *et al.*, *eLife* **5**, e12444 (2016).
36. J. Martinez *et al.*, *Nat. Cell Biol.* **17**, 893–906 (2015).
37. J. L. Round *et al.*, *Science* **332**, 974–977 (2011).
38. M. A. Sanjuan *et al.*, *Nature* **450**, 1253–1257 (2007).
39. Wellcome Trust Case Control Consortium, *Nature* **447**, 661–678 (2007).
40. C. D. Packey, R. B. Sartor, *Curr. Opin. Infect. Dis.* **22**, 292–301 (2009).
41. N. A. Molodecky *et al.*, *Gastroenterology* **142**, 46–54.e42, quiz e30 (2012).

ACKNOWLEDGMENTS

We thank L. Hwang, E. Park, and M. Salas for clinical research coordination (Cedars-Sinai); A. Maskell, L. Sandoval, and C. Rumaldo for animal husbandry (Caltech); and members of the Mazmanian laboratory for discussions and critical reading of the manuscript. The data presented in this manuscript are tabulated in the main paper and in the supplementary materials. This work was supported by the National Institutes of Health (NIH) under a Ruth L. Kirschtein National Research Service Award (DK100109) to H.C.; NIH DK097485 to R.J.X.; NIH PO1DK046763, the Cedars-Sinai F. Widjaja Foundation Inflammatory Bowel and Immunobiology Research Institute Research Funds, and The Feintech Family Chair in IBD to S.R.T.; Wayne and Gladys Valley Foundation and NIH AI079145 to P.B.E.; The Lupus Research Institute and NIH AI40646 to D.R.G; NIH U19 AI109725 to H.W.V.; The Lisa Z. Greer Endowed Chair in IBD Genetics, NIH DK062413, NIH DE023789-01, grant 305479 from the European Union, The Crohn's and Colitis Foundation of America, and The Leona M. and Harry B. Helmsley Charitable Trust to D.P.B.M.; NIH AI109725 to H.W.V.; and NIH DK078938, NIH GM099535, The Crohn's and Colitis Foundation of America, and the Heritage Medical Research Institute to S.K.M. Rubicon and ULK1 knockout mice were obtained from D. R. Green and M. Kundu, respectively, under a materials transfer agreement with St. Jude Children's Research Hospital. A provisional patent application entitled "Beneficial Activation of Autophagy Components by the Microbiome" has been filed by H.C., H.W.V., and S.K.M.

SUPPLEMENTARY MATERIALS

www.sciencemag.org/content/352/6289/1116/suppl/DC1
Materials and Methods
Figs. S1 to S18
Table S1
References (*42*–*47*)

3 December 2015; accepted 21 April 2016
Published online 5 May 2016
10.1126/science.aad9948

Science

Gene-microbiota interactions contribute to the pathogenesis of inflammatory bowel disease

Hiutung Chu, Arya Khosravi, Indah P. Kusumawardhani, Alice H. K. Kwon, Anilton C. Vasconcelos, Larissa D. Cunha, Anne E. Mayer, Yue Shen, Wei-Li Wu, Amal Kambal, Stephan R. Targan, Ramnik J. Xavier, Peter B. Ernst, Douglas R. Green, Dermot P. B. McGovern, Herbert W. Virgin and Sarkis K. Mazmanian

Science **352** (6289), 1116-1120.
DOI: 10.1126/science.aad9948originally published online May 5, 2016

Genes and microbes converge in colitis

Both host genetics and intestinal microbes probably contribute to a person's overall susceptibility to inflammatory bowel disease (IBD). The human gut microbe *Bacteroides fragilis* produces immunomodulatory molecules that it releases via outer membrane vesicles (OMVs). These molecules can protect mice from experimentally induced colitis. Chu *et al.* now find that OMV-mediated protection from colitis requires *Atg16l1* and *Nod2* genes whose human orthologs are associated with an increased risk for developing IBD. OMVs trigger an ATG16L1 and NOD2–dependent noncanonical autophagy pathway in dendritic cells (DCs). OMV-primed DCs, in turn, induce regulatory T cells in the intestine that protect against colitis.

Science, this issue p. 1116